Site-Specific Patterning of Highly Ordered Nanocrystal Superlattices through Biomolecular Surface Confinement

Hyunwoo Noh,[†] Chulmin Choi,[‡] Albert M. Hung,[†] Sungho Jin,[†,‡] and Jennifer N. Cha[†,*]

[†]Department of Nanoengineering and [‡]Department of Mechanical and Aerospace Engineering and University of California, San Diego, 9500 Gilman Drive, La Jolla, California 92093

ABSTRACT With the increasing demand in recent years for high-performance devices for both energy and health applications, there has been extensive research to direct the assembly of nanoparticles into meso- or macroscale single two- and three-dimensional crystals of arbitrary configuration or orientation. Inorganic nanoparticle arrays can have intriguing physical properties that differ from either individual nanoparticles or bulk materials. For most device applications, it is necessary to fabricate two-dimensional nanoparticle superlattices at programmed sites on a surface. However, it has remained a significant challenge to generate patterned arrays with long-range positional order because most highly ordered close-packed nanocrystal arrays are typically obtained by kinetically driven evaporation processes. In this report, we demonstrate a method to generate patterned nanocrystal superlattices by confining nanoparticles to geometrically defined 2-D DNA sites on a surface and using associative biomolecular interparticle interactions to produce thermodynamically stable arrays of hexagonally packed nanocrystals with significant long-range order observed over $1-2$ μm. We also demonstrate the role of chemical and geometrical confinement on particle packing and obtaining long-range order. Finally, we also demonstrate that the formation of DNA-mediated nanocrystal superlattices requires both interparticle DNA hybridization and solvent-less thermal annealing.

KEYWORDS: nanocrystal · DNA · self-assembly · superlattice

*Address correspondence to jencha@ucsd.edu.

The ability to direct the assembly of single or multicomponent nanoparticles into meso- or macroscale single two- and three-dimensional crystals of any desired configuration, orientation, and geometry is currently of significant interest for high-powered applications in both energy and health.[1−14] While the properties of nanomaterials of varying composition, size, and morphology can be tuned easily, it has remained a daunting task to hierarchically assemble nanocrystals with perfect or near-perfect long-range order in both two and three dimensions at predefined sites on a substrate.[15,16] Methods to engineer patterned 2-D nanocrystal superlattices of arbitrary feature size, pitch, and density have remained elusive because highly ordered close-packed nanocrystal arrays are typically obtained by kinetically driven evaporation processes, which produce local order but limited long-range positional order.[5,17−19] To arrange organic and inorganic materials into programmed assemblies with precision and order, Nature both sequesters the raw materials into confined spaces and encourages their association through highly specific noncovalent interactions between biomolecules. We demonstrate here that similar strategies can be employed by confining nanoparticles to geometrically defined 2-D DNA sites on a surface and using biomolecular associative interparticle interactions to generate thermodynamically stable arrays of hexagonally packed nanocrystals with significant long-range order observed over $1-2$ μm. We furthermore show that chemically immiscible boundaries at the edges of each nanocrystal array strongly influence particle packing and ordering; as the 2-D DNA features decrease in size from 3 μm to 200 nm, 60° parallelogram DNA patterns promoted long-range order of hexagonally packed particles but square DNA arrays generated largely disordered arrangements. In this report, we also demonstrate that obtaining long-range order within a nanocrystal superlattice requires both interparticle DNA hybridization and solvent-less thermal annealing above the melting temperatures (T_m) of the DNA strands.

RESULTS AND DISCUSSION

To confine particles specifically to geometrically defined sites on a substrate, arrays of micro- and mesoscale features of DNA, oligonucleotides were first prepared on silicon oxide using a modified version of a previously developed subtraction print-

ing process (Figure 1).[20] By subtraction printing twice on two separate silicon masters, 2-D DNA patterns could be generated that encode sharp edges and corners with sub-200 nm resolution, which are typically difficult to obtain by conventional photolithography or e-beam lithography. In order to minimize the thickness of the DNA arrays, all of the polydimethylsiloxane (PDMS) substrates were inked with 20 pmol of polyadenine (A_{15}) to produce DNA features 4−5 nm in height, corresponding to about 1−2 layers of A_{15}. Next, as a means to confine nanoparticles to the DNA arrays and discourage their association outside of the patterned domain, the remaining exposed silicon surfaces were covalently modified with hexyltrimethoxysilane (HTS) by vapor phase silylation for 15 h at 45 °C.[21,22] Contact angle and ellipsometry measurements of bare silicon substrates exposed to HTS after 15 h confirmed sufficient surface treatment to generate a highly hydrophobic surface. Through ellipsometry and AFM scratch measurements, the film thickness was determined to be between 0.769 and 0.8 nm and showed a water contact angle of 78.2°.

After HTS surface treatment, 100 nM solutions of polythymine (T_{15})-conjugated 10 nm gold nanocrystals were adsorbed onto the printed polyadenine (A_{15}) substrates, followed by ethanol rinsing to remove excess gold and salts. After these steps, since the gold solutions had only been in contact with the substrate for 5 min, the assembled particles were largely disordered with respect to each other, and neither local nor long-range order was seen (Supporting Information Figure 1). To allow the nanoparticles to reach their equilibrium state, the samples were next subjected to thermal annealing in a humid environment at 60 °C—above the T_m of the DNA—for 4−5 h. Annealing in this manner promoted particle mobility while minimizing the risk of particle removal due to the presence of bulk solvent.

As shown in Figure 2A, after thermal annealing in saturated water vapor for 5 h, extremely well-ordered arrays of hexagonally packed nanoparticle superlattices were observed within each patterned parallelogram array. As will be discussed later, nanocrystal hexagonal packing was most likely due to some of the surface-bound A_{15} strands acting as bridging linkers between T_{15} strands on neighboring particles. While the nanocrystal packing within 3 μm square DNA features also showed a fair amount of order, in general, many more grain boundaries were observed, and the edges of the square gold nanocrystal arrays were not well-defined or as sharp as those observed with the parallelogram patterns (Figure 2B). By imaging a roughly 1.5 μm area within a single parallelogram nanoparticle array, the gold nanoparticles were found to tightly pack into a well-ordered 2-D hexagonal superlattice. Fourier transforms (FT) of selected areas within the 1.5 μm domain show that the rotation of the superlattice over this im-
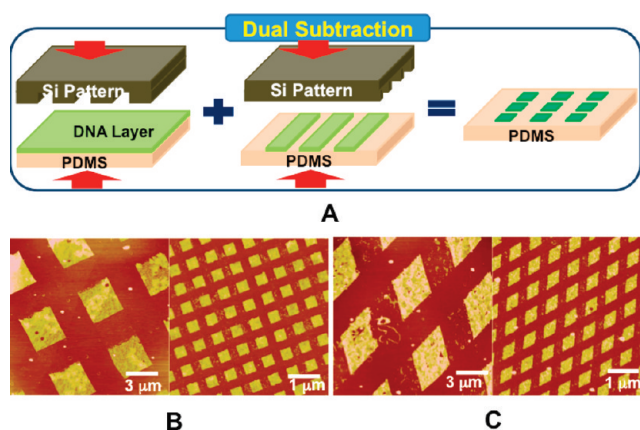

Figure 1. (A) Schematic of double subtraction method used to generate 2-D features of DNA on PDMS. (B) AFM images of 3 μm and 400 nm squares generated by double subtraction and printing. (C) AFM images of 3 μm and 400 nm parallelograms generated by double subtraction and printing.

age area varied by no more than ±7° (relative to area IV), confirming strong long-range positional order (Figure 3).

While it appears that the combination of interparticle DNA hybridization and thermal annealing allowed for the formation of highly ordered superlattice nanocrystal arrays, the role that particle confinement and the hydrophobic boundaries surrounding each DNA pattern play on nanocrystal packing and ordering remains less clear. When large micrometer sized features of DNA are used for the assembly process, it is difficult to discern the roles of the boundaries since any effect they may have on particle packing and ordering is mitigated at locations far from the edge. However, as the DNA patterns decrease in size, the boundary edges and corners should begin to have a dominating effect if there is in fact strong chemical confinement. These forces might even be strong enough to prevent the energetically favored nanocrystal hexagonal packing seen thus far such that while long-range order might be obtained on smaller parallelogram DNA patterns, mainly disordered arrays of particles would be seen on the DNA squares.

In order to test the effect of strong geometric chemical confinement on nanocrystal ordering, ∼200 nm mesoscale parallelogram and square features of A_{15} were first patterned on silicon as described above. Next, as with the micrometer DNA features, T_{15}-conjugated gold nanocrystals were added followed by ethanol rinsing to remove excess salts and nanocrystals. All of the gold arrays were subsequently subjected to thermal annealing at 60 °C for 5 h. As is shown clearly in Figure 4A, the sequestration of gold nanocrystals to the roughly 200 nm parallelogram features of DNA within the HTS monolayer was enough to drive both local hexagonal packing of 10 nm gold nanocrystals as well as good long-range positional order. Fourier transform
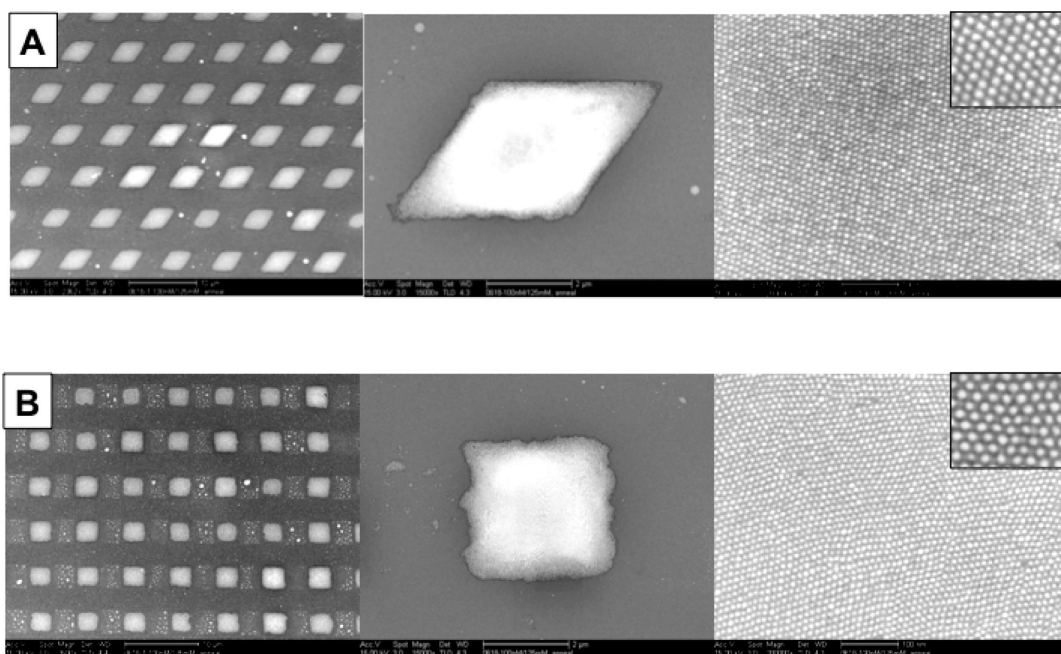
Figure 2. Low- and high-magnification SEM images of nanocrystal superlattices obtained after adsorbing and annealing T_{15}-conjugated gold to (A) 3 μm parallelogram and (B) 3 μm square patterns of A_{15}.

analysis of an image of an individual ~200 nm parallelogram nanoparticle array in its entirety yielded six diffuse spots, quantitatively demonstrating partial orientation order within the 200 nm superlattice. In contrast, T_{15}-conjugated gold nanocrystals patterned on the 200 nm square A_{15} domains showed completely disordered arrangements (Figure 4B).

Because the DNA sequences, nanoparticle concentrations, annealing temperatures, and times were all held exactly the same, the only reason disorder would be observed within the square arrays and not the parallelograms is that the edge and corner boundaries of the mesoscale DNA patterns place a significant constraint to prevent any particle migration or association with the neighboring hydrophobic HTS areas. Although it should be noted that the overall edge roughness and corner sharpness of the

200 nm square and parallelogram nanoparticle arrays are weak, highly ordered packing is still not observed even in larger 400 nm square arrays where edge roughness and corner rounding should be less influential (Supporting Information Figure 2). This is most likely because, even with a perfectly shaped 90° corner, the sides of a square would favor two competing hexagonally close-packed (hcp) orientations rotated 30° with respect to each other. While with very large squares, this would result in multiple grains and grain boundaries, in smaller squares these grain boundary defects will most likely occupy the majority of the packed nanoparticle area. Therefore, despite the strong tendency of the particles to pack into hcp arrays as observed within the parallelogram features, the boundaries of the square DNA domains drove disorder toward the energetically unfavorable non-hcp orientations. The clear difference in packing and ordering observed between the two different patterned DNA geometries demonstrates the strong confinement effect the chemically immiscible boundaries have on particle sequestration and orientation and their importance toward obtaining long-range order within close-packed nanocrystal arrays.

In order to demonstrate that the observed hexagonal packing of the nanoparticles was due to interparticle hybridization mediated by the A_{15} strands, T_{10}-AAGACGAATATTTAACAA (DNA-1) conjugated 10 nm gold was adsorbed to 3 μm parallelogram arrays of the DNA oligonucleotide A_{10}-TTCTGCTTATAAATTGTT
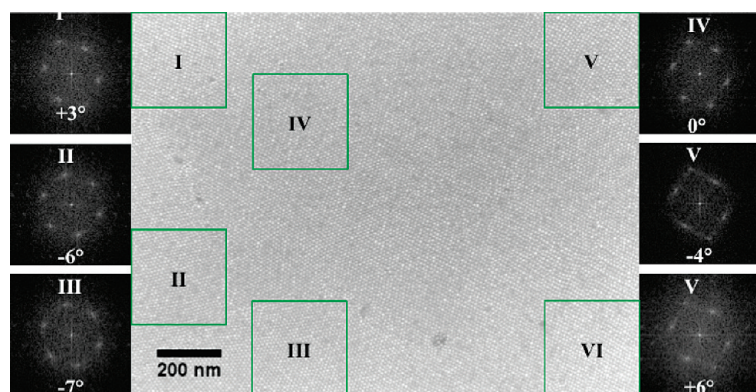

Figure 3. SEM image of a 1.5 μm area within a single parallelogram nanocrystal array. The gold nanoparticles are tightly packed in a 2-D hexagonal superlattice. Fourier transforms of selected areas show that the rotation of the superlattice over this image area varies by no more than ±7° (relative to area IV).
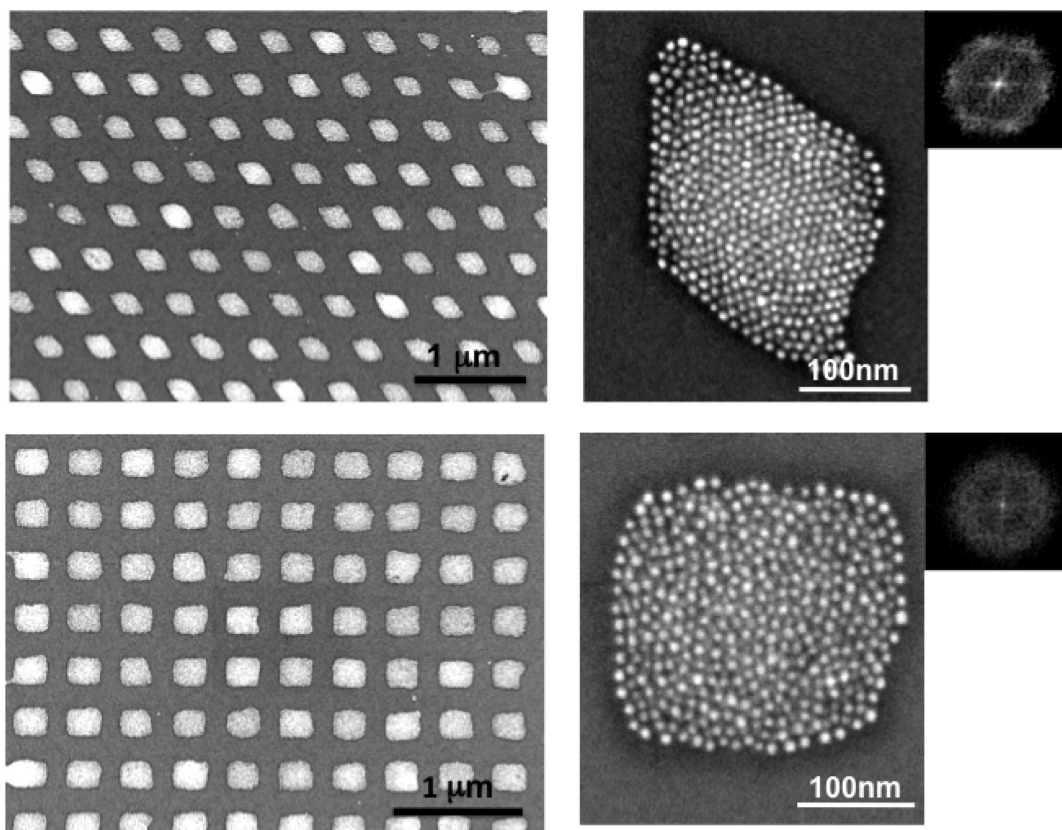
Figure 4. Low- and high-magnification SEM images of nanocrystal superlattices obtained after adsorbing and annealing T_{15}-conjugated gold to (top) 200 nm parallelogram and (bottom) 200 nm square patterns of A_{15}. Insets show FTs of a ~200 nm parallelogram and 200 nm square nanocrystal array, each in its entirety.

(cDNA-1). Because, in this case, a strand of DNA on the surface can only hybridize to one strand on any given particle, no DNA-assisted inteparticle bridging can occur. Using the exact same assembly conditions as the T_{15} and A_{15} systems, nanocrystal arrays from the DNA-1 and cDNA-1 sequences appeared to be largely disordered with very limited local order (Supporting Information Figure 3). Because very minimal hexagonal packing was seen in this case, it is clear that hexagonal ordering was not caused by the physical entrapment of gold nanocrystals to a given domain but rather that the crystallographic orientation was thermodynamically driven, with multiple A_{15} strands acting as DNA linkers to drive interparticle association. These interactions would be caused either by substrate-bound DNA or desorbed DNA hybridizing to two separate strands on neighboring gold nanoparticles. When a strand of DNA on the surface can only hybridize to a single strand on an individual particle, there is no interparticle attractive force to drive assembly, resulting largely in disordered arrangements.

CONCLUSIONS

In conclusion, we demonstrate here that, by combining particle sequestration and confinement with interparticle attractive forces with thermal annealing, it is possible to obtain thermodynamically stable, well-defined nanoparticle superlattices that show long-range positional order at specific, predetermined sites on a substrate. We furthermore show that strong confinement effects can be induced simply by having chemically immiscible boundaries at the edges of each nanocrystal array and that these can strongly influence particle packing and ordering. The work shown thus far demonstrates the first lessons toward obtaining highly ordered 2-D and 3-D nanoparticle structures in a deterministic and controllable fashion, and these will be applied in future studies toward engineering more complex nanocrystal arrangements that show different crystallographic orientations or are composed of multiple types of nanocrystal materials.

MATERIALS AND METHODS

Silicon Patterns. Silicon line patterns of 200 and 400 nm dimensions were fabricated as published.[23] The micrometer sized Si templates were obtained from a photolithographically patterned

(100) silicon wafer (Ultrasil Corp.) and a reactive ion etch (RIE). A positive photoresist was first spin-coated on the silicon wafer followed by exposure using a a Karl Suss MA6Mask Aligner system to create the patterned lines. After exposure and development, a

2 μm thick mask was used to transfer the line patterns into silicon by RIE using a SF_6/C_4F_8 mixture gas.

DNA Patterning. All silicon substrates were cleaned by sonication in acetone, ethanol, and DI water successively. PDMS substrates were cleaned by sonication in ethanol and DI water. Both PDMS and Si substrates were next rendered hydrophilic by UVO (Jelight, model 42) treatment with 3 SCFH oxygen gas. UVO-treated PDMS substrates were inked with 1 μL of 20 μM polyadenine(A_{15}) (Integratred DNA Technologies) and incubated in a humid chamber for 30 min. The DNA-inked PDMS substrates were then briefly blown dry with nitrogen. Each subtraction printing step was performed by loading a 50 g weight on top of the PDMS, bringing it into contact with the silicon master for 30 s. DNA-patterned Si substrates were next vapor treated with hexyltrimethoxysilane (Gelest Inc.) in a 45 °C oven.

Conjugation of AuNP—DNA. Ten nanometer gold nanoparticles (Ted Pella) first reacted with bis(p-sulfonatophenyl)phenyl-phosphine dihydrate dipotassium salt (Strem Chemicals) and concentrated according to ref 24. The phosphine-stabilized nanoparticles were then mixed with 5′-thiolated polythymine (T_{15}) using 200:1 molar ratios of DNA to gold and incubated for at least 12 h. Excess salts and DNA were removed by washing particle solutions out three times using a 30 kDa MWCO centrifuge filter (NANOSEP, Pall Corp.). Nanoparticles were resuspended in DI water and kept stored in a refrigerator at 4−8 °C.

AuNP Hybridization. Six microliters of DNA-conjugated gold nanoparticle solution with $MgCl_2$ was dropped onto a DNA-patterned Si substrate and absorbed for 5 min. To remove excess AuNPs and salts, the substrates were next briefly dipped in the solutions of 125 mM Mg in 1× TAE buffer followed by a 5 s 50% ethanol rinse and a 30 min immersion in 90% ethanol. Thermal annealing of the gold nanoparticle arrays was done by heating the substrates at 60 °C in a humid environment for 4−5 h.

Supporting Information Available: Additional figures. This material is available free of charge *via* the Internet at http://pubs.acs.org.

REFERENCES AND NOTES

1. Murray, C. B.; Kagan, C. R.; Bawendi, M. G. Self-Organization of CdSe Nanocrystallines into 3-Dimensional Quantum-Dot Superlattices. *Science* **1995**, *270*, 1335–1338.
2. Zhao, Y.; Thorkelsson, K.; Mastroianni, A. J.; Schilling, T.; Luther, J. M.; Rancatore, B. J.; Matsunaga, K.; Jinnai, H.; Wu, Y.; Poulsen, D.; *et al.* Small-Molecule-Directed Nanoparticle Assembly towards Stimuli-Responsive Nanocomposites. *Nat. Mater.* **2009**, *8*, 979–985.
3. Rosi, N. L.; Mirkin, C. A. Nanostructures in Biodiagnostics. *Chem. Rev.* **2005**, *105*, 1547–1562.
4. Perrault, S. D.; Chan, W. C. W. *In Vivo* Assembly of Nanoparticle Components To Improve Targeted Cancer Imaging. *Proc. Natl. Acad. Sci. U.S.A.* **2010**, *107*, 11194–11199.
5. Cheng, W.; Campolongo, M. J.; Cha, J. J.; Tan, S. J.; Umbach, C. C.; Muller, D. A.; Luo, D. Free Standing Nanoparticle Superrlattice Sheets Controlled by DNA. *Nat. Mater.* **2009**, *8*, 519–525.
6. Gur, I.; Fromer, N. A.; Geier, M. L.; Alivisatos, A. P. Air-Stable All-Inorganic Nanocrystal Solar Cells Processed from Solution. *Science* **2005**, *310*, 462–465.
7. Velev, O. D.; Gupta, S. Materials Fabricated by Micro- and Nanoparticle Assembly: The Challenging Path from Science to Engineering. *Adv. Mater.* **2009**, *21*, 1897–1905.
8. Cheng, M. M.-C.; Cuda, G.; Bunimovich, Y. L.; Gaspari, M.; Heath, J. R.; Hill, H. D.; Mirkin, C. A.; Nijdam, A. J.; Terracchiano, R.; Thundat, T.; *et al.* Nanotechnologies for Biomolecular Detection and Medical Diagnostics. *Curr. Opin. Chem. Biol.* **2006**, *10*, 11–19.
9. Tang, Z.; Zhang, Z.; Wang, Y.; Glotzer, S. C.; Kotov, N. A. Self-Assembly of CdTe Nanocrystals into Free-Floating Sheets. *Science* **2006**, *314*, 274–278.
10. Ryeenga, M.; McLellan, J. M.; Xia, Y. Controlling the Assembly of Silver Nanocubes through Selective Functionalization of Their Faces. *Adv. Mater.* **2008**, *20*, 2416–2420.
11. Taton, T. A.; Mirkin, C. A.; Letsinger, R. L. Scanometric DNA Array Detection with Nanoparticle Probes. *Science* **2000**, *289*, 1757–1760.
12. Park, S. Y.; Lytton-Jean, A. K. R.; Lee, B.; Weigand, S.; Schatz, G. C.; Mirkin, C. A. DNA-Programmable Nanoparticle Crystallization. *Nature* **2008**, *451*, 553–556.
13. Nykypanchuk, D.; Maye, M. M.; van der Lelie, D.; Gang, O. DNA-Guided Crystallization of Colloidal Nanoparticles. *Nature* **2008**, *451*, 549–552.
14. Ferrari, M. Cancer Nanotechnology: Opportunities and Challenges. *Nat. Rev. Cancer* **2005**, *5*, 161–171.
15. Kannan, B.; Kulkarni, R. P.; Majumdar, A. DNA-Based Assembly of Gold Nanoparticles on Lithographic Patterns with Extraordinary Specificity. *Nano Lett.* **2004**, *4*, 1521–1524.
16. Cui, Y.; Björk, M. T.; Liddle, J. A.; Sönnichsen, C.; Boussert, B.; Alivisatos, A. P. Integration of Colloidal Nanocrystals into Lithographically Patterned Devices. *Nano Lett.* **2004**, *4*, 1093–1098.
17. Cheng, W.; Park, N.; Walter, M. T.; Hartman, M. R.; Luo, D. Nanopatterning Self-Assembled Nanoparticle Superlattices by Moulding Microdroplets. *Nat. Nanotechnol.* **2008**, *3*, 682–690.
18. Mueggenburg, K. E.; Lin, X.-M.; Goldsmith, R. H.; Jaeger, H. M. Elastic Membranes of Close-Packed Nanoparticle Arrays. *Nat. Mater.* **2007**, *6*, 656–660.
19. Shevchenko, E. V.; Talapin, D. V.; Kotov, N. A.; O'Brien, S.; Murray, C. B. Structural Diversity in Binary Nanoparticle Superlattices. *Nature* **2006**, *439*, 55–59.
20. Noh, H.; Hung, A. M.; Choi, C.; Lee, J. H.; Kim, J.-Y.; Jin, S.; Cha, J. N. 50 nm DNA Nanoarrays Generated from Uniform Oligonucleotide Films. *ACS Nano* **2009**, *3*, 2376–2382.
21. Kershner, R. J.; Bozano, L. D.; Micheel, C. M.; Hung, A. M.; Fornof, A. R.; Cha, J. N.; Rettner, C. T.; Bersani, M.; Frommer, J; Rothemund, P. W. K.; *et al.* Placement and Orientation of Individual DNA Shapes on Lithographically Patterned Surfaces. *Nat. Nanotechnol.* **2009**, *4*, 557–561.
22. Hung, A. M.; Micheel, C. M.; Bozano, L. D.; Osterbur, L. W.; Wallraff, G. M.; Cha, J. N. Large-Area Spatially Ordered Arrays of Gold Nanoparticles Directed by Lithographically Confined DNA Origami. *Nat. Nanotechnol.* **2010**, *5*, 121–126.
23. Park, J.; Chen, L.-H.; Hong, D.; Choi, C.; Loya, M.; Brammer, K.; Bandaru, P.; Jin, S. Geometry Transformation and Alterations of Periodically Patterned Si Nanotemplates by Dry Oxidation. *Nanotechnology* **2009**, *20*, 015303.
24. Loweth, C. J.; Caldwell, W. B.; Peng, X.; Alivisatos, A. P.; Schultz, P. G. DNA-Based Assembly of Gold Nanocrystals. *Angew. Chem., Int. Ed.* **1999**, *38*, 1808–1812.